Journal of Chemical Ecology (2018) 44:1101–1114
https://doi.org/10.1007/s10886-018-1029-y

Desiccation Resistance and Micro-Climate Adaptation: Cuticular Hydrocarbon Signatures of Different Argentine Ant Supercolonies Across California

Jan Buellesbach[1,2] · Brian A. Whyte[1] · Elizabeth Cash[1] · Joshua D. Gibson[1,3] · Kelsey J. Scheckel[1] · Rebecca Sandidge[1] · Neil D. Tsutsui[1]

Received: 31 May 2018 / Revised: 1 October 2018 / Accepted: 23 October 2018 / Published online: 15 November 2018

Abstract

Cuticular hydrocarbons (CHCs), the dominant fraction of the insects' epicuticle and the primary barrier to desiccation, form the basis for a wide range of chemical signaling systems. In eusocial insects, CHCs are key mediators of nestmate recognition, and colony identity appears to be maintained through a uniform CHC profile. In the unicolonial Argentine ant *Linepithema humile*, an unparalleled invasive expansion has led to vast supercolonies whose nestmates can still recognize each other across thousands of miles. CHC profiles are expected to display considerable variation as they adapt to fundamentally differing environmental conditions across the Argentine ant's expanded range, yet this variation would largely conflict with the vastly extended nestmate recognition based on CHC uniformity. To shed light on these seemingly contradictory selective pressures, we attempt to decipher which CHC classes enable adaptation to such a wide array of environmental conditions and contrast them with the overall CHC profile uniformity postulated to maintain nestmate recognition. *n*-Alkanes and *n*-alkenes showed the largest adaptability to environmental conditions most closely associated with desiccation, pointing at their function for water-proofing. Trimethyl alkanes, on the other hand, were reduced in environments associated with higher desiccation stress. However, CHC patterns correlated with environmental conditions were largely overriden when taking overall CHC variation across the expanded range of *L. humile* into account, resulting in conserved colony-specific CHC signatures. This delivers intriguing insights into the hierarchy of CHC functionality integrating both adaptation to a wide array of different climatic conditions and the maintenance of a universally accepted chemical profile.

Keywords Nestmate recognition · Chemical communication · Water-proofing · *Linepithema humile* · Invasive species · *n*-alkanes · *n*-alkenes · Methyl-branched alkanes · Gas chromatography · Mass spectrometry

Introduction

Varied interactions with the physical environment often have direct consequences on the fitness of an organism and, by extension, can be a crucial factor for species survival, particularly in novel environments (Burger and Lynch 1995; Gomulkiewicz and Holt 1995). Introduced species are often exposed to environments vastly different to their native range, and those with the ability to withstand the novel conditions may establish persistant populations (Clavero and García-Berthou 2005). The natural history and physical characteristics of introduced species determine how it can survive and successfully establish itself in novel environments (Kolar and Lodge 2001). Organisms with small body sizes, for example, possess a higher surface area to volume ratio than larger organisms, increasing the importance of mediating homeostasis across the boundary that divides the internal body from the environment (Jackson and Baker 1969; Gibbs 1998). In terrestrial environments, organisms are typically surrounded by air that is much drier than their internal, liquid-rich tissues and organs, rendering the prevention of desiccation pivotal for their survival (Chown et al. 2011; Schilman et al. 2005).

Electronic supplementary material The online version of this article (https://doi.org/10.1007/s10886-018-1029-y) contains supplementary material, which is available to authorized users.

✉ Jan Buellesbach
buellesb@uni-muenster.de

[1] Department of Environmental Science, Policy, & Management, University of California, 130 Mulford Hall #3114, Berkeley, CA 94720, USA

[2] Institute for Evolution and Biodiversity, University of Münster, Hüfferstr. 1, 48149 Münster, Germany

[3] Department of Biology, Georgia Southern University, P.O. Box 8042-1, Statesboro, GA 30460, USA

In insects, one major barrier to desiccation is the waxy film of hydrocarbons that coats their cuticle (Gibbs 1998; Hadley 1981). Common cuticular hydrocarbon (CHC) classes include linear *n*-alkanes, linear *n*-alkenes, and methylated alkanes (Blomquist and Bagnères 2010; Gibbs 1995). Other CHC classes, such as alkadienes or methylated alkenes, occur more rarely in insect CHC profiles (Blomquist et al. 1987; Martin and Drijfhout 2009). CHC chain lengths generally vary between 20 and 40 carbon atoms, and previous studies have indicated that their efficacy in preventing desiccation increases with carbon chain length (Gibbs and Pomonis 1995; Gibbs et al. 1997; Rouault et al. 2004). In addition, different types of CHCs have different physical properties, and therefore vary in efficacy as barriers to water loss. The melting temperature (T_m) of a particular hydrocarbon, for example, is a crucial property because the transition from solid to liquid results in a substantial increase in cuticular permeability, and consequently, water loss (Gibbs 2002; Gibbs and Rajpurohit 2010). Previous research has revealed some general principles on CHC properties: 1) Unbranched alkanes have the highest T_m (increasing by 1–3 °C with each additional carbon), 2) T_m is substantially reduced (by 20–50 °C) when CHCs possess double bonds or methyl branches (Gibbs and Pomonis 1995; Gibbs and Rajpurohit 2010). Thus, we would generally expect higher proportions of CHC classes with higher T_m and thus more efficient water-proofing in drier habitats characterized by high temperature and low precipitation rates, and more flexible CHC profile variation in more temperate habitats (e.g., Chown et al. 2011; Gefen et al. 2015; Hadley 1981).

The Argentine ant, *Linepithema humile*, is a widespread and damaging invader and is listed by the International Union for Conservation of Nature (IUCN) as one of the world's 100 most damaging invasive species (Lowe et al. 2004). Argentine ants were introduced to North America in 1891 and had become established by 1907 in California (Suarez et al. 2001). The Argentine ant possesses radically different forms of social organization in its native and introduced ranges (Tsutsui et al. 2000; Tsutsui and Case 2001). In the native range, colonies occupy well-defined, spatially discrete territories, typically tens to hundreds of meters in diameter, that are aggressively defended against other Argentine ant colonies (Pedersen et al. 2006; Suarez et al. 1999; Tsutsui et al. 2000; Tsutsui and Case 2001). In contrast, introduced populations of Argentine ants are *unicolonial* (Markin 1970; Newell and Barber 1913; Tsutsui et al. 2000; Tsutsui and Case 2001), forming vastly expanded supercolonies that lack territory boundaries. The success of Argentine ants in their introduced range is a direct result of their unicolonial structure. Reductions in aggression and intraspecific competition eliminate many costs associated with these behaviors, such as mortality caused by aggression, allowing populations to achieve high densities (Holway et al. 1998). In introduced populations, genetic homogenization has resulted in concomitant homogenization of recognition cues and, in turn, the formation of spatially widespread supercolonies (Tsutsui et al. 2000; Tsutsui and Case 2001).

Despite the unusual form of social organization in introduced populations, the mechanism for colonymate recognition in Argentine ants is similar to that of other ants. Workers use CHC profiles to distinguish between nestmates (self) and non-nestmates (non-self) (Brandt et al. 2009; Suarez et al. 2002; Torres et al. 2007). In Argentine ants, CHC variation appears to have a genetic basis: Genetically similar ants, originating from the same supercolony, have similar CHC profiles and are not aggressive towards each other, whereas genetically different ants possess different CHC profiles and display high levels of aggression towards each other (Brandt et al. 2009; Suarez et al. 2002; Tsutsui et al. 2000, 2001; Tsutsui and Suarez 2003). Although a single, "main" supercolony occupies almost all of the introduced range in California, several smaller, genetically different "secondary" supercolonies also occur in Southern California and display aggression between themselves and the main super colony, not recognizing ants of the other supercolonies as nestmates (Suarez et al. 1999; Tsutsui et al. 2000; Tsutsui and Case 2001; Tsutsui et al. 2003). We have previously discovered, synthesized, and behaviorally verified many of the specific CHCs that are used for nestmate recognition between these colonies (Brandt et al. 2009; van Wilgenburg et al. 2010, 2012). We have shown that important structural features of key CHCs for colonymate recognition are the numbers and positions of methyl-branchings, whereas the carbon chain length appears to be less important (van Wilgenburg et al. 2010).

Interestingly, Argentine ants are particularly sensitive to desiccation. The availability of water limits their geographic range and expansion into new habitats, and Argentine ants are more sensitive to desiccation than the native ants they displace in their introduced range (Schilman et al. 2005). Here, we present results from a study of Argentine ants that correlates CHC variation with climatic factors across geographically distant sites over California that belong to the same main supercolony as well as to behaviorally and genetically different secondary supercolonies. We compare variation in the identified CHC classes between different *L. humile* populations in relation to environmental conditions they are expected to encounter in their different habitats, in order to contrast and identify colony-, habitat-, and season-specific CHC signatures.

Methods and Materials

Colony Sampling and Maintenance Argentine ant colonies were collected at different time points during the first half of 2017 (Fig. 1). Collection sites from the main California supercolony were Albany Bulb (AB, lat: 37.89013, long:

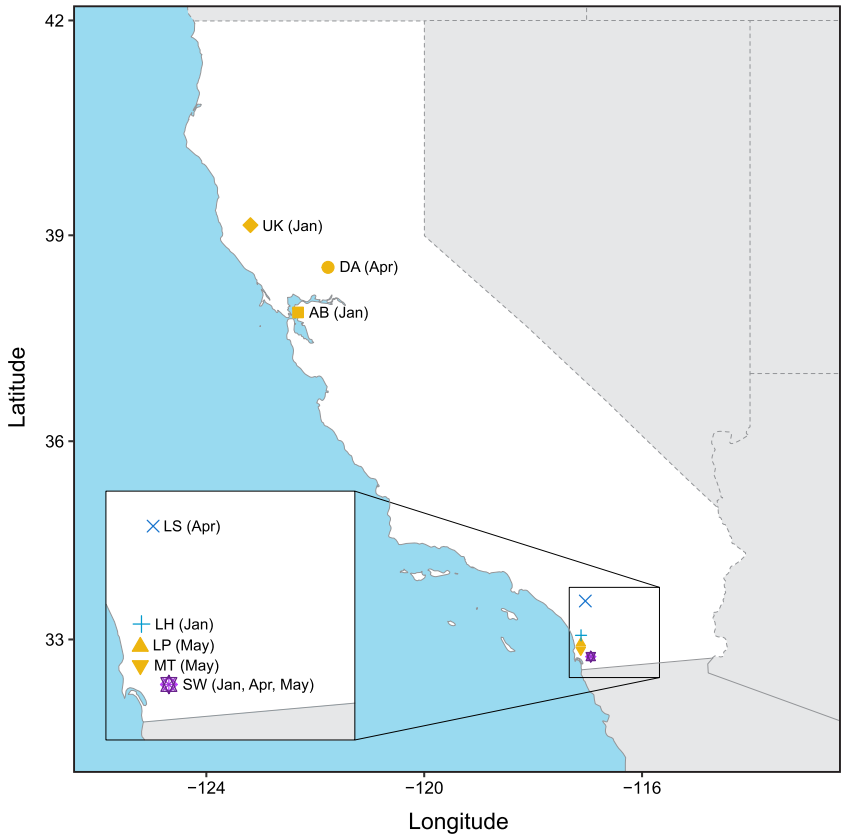

Fig. 1 Map of California displaying the sample locations for the different *L. humile* supercolony populations investigated in this study. Longitudinal and latitudinal data are displayed on the x- and y-axis, respectively. Acronyms for *L. humile* populations of the main supercolony are AB: Albany Bulb, DA: Davis, UK: Ukiah, LP: Los Peñasquitos and MT: Mission Trails, indicated by different symbols in gold. Acronyms for *L. humile* populations of the secondary supercolonies are LH: Lake Hodges, LS: Lake Skinner and SW: Sweetwater, indicated by different in symbols in shades of blue and violet. Sampling months are indicated in parentheses, note that Sweetwater was sampled at all three sampling months as a seasonal control

−122.3163, collected in January), Ukiah (UK, lat: 39.14607, long: −123.19234, January), Davis (DA, lat: 38.54258, long: −121.76567, April), Mission Trails (MT, lat: 32.84006, long: −117.12647, May) and Los Peñasquitos (LP, lat: 32.93845, long: −117.12979, May). Collection sites from the "secondary" supercolonies in southern California were Lake Hodges (LH, lat: 33.06271, long: −117.11886, January), Lake Skinner (LS, lat: 33.58876, long: −117.04138, April) and Sweetwater (SW, lat: 32.73395, long: −116.94099, January, April, and May), with the latter one being sampled at all three time points to control for seasonal variation.

At least 500 workers, including multiple queens, were collected at each site and subsequently kept as stock laboratory colonies to facilitate sampling for future experiments. In the field, ants were collected from nesting substrate, such as dead wood and earth, using trowels, and then placed into 5 gal plastic buckets (Home Depot Inc., Atlanta, Georgia, USA). All buckets were coated with PTFE Fluoropolymer (Insect-a-slip, BioQuip Products, Rancho Dominguez, California, USA) to prevent the ants from escaping. At the laboratory, the contents of the buckets including the collected ants and nest substrates were emptied into separate 27 L plastic storage bins (58.4 cm × 41.3 cm × 15.2 cm, Sterilite, Townsend, Massachusetts, USA) that were also coated with PTFE Fluoropolymer. Ants were allowed to acclimate overnight in storage bins with nest materials and covered with water-moistened paper towels to prevent them from drying out. New, clean 27 L bins were set up as permanent nests containing 4–6 water-filled glass test tubes (18 mm × 150 mm) plugged with cotton (Fisher Scientific, Pittsburgh, Pennsylvania, USA) and 4–6 plastic Petri dishes (100 mm × 15 mm) drilled with a small hole (3 mm diameter) and filled 0.5 cm deep with cured plaster-of-Paris. The new nest bins were connected to the bins containing the collected ants and the nesting material via paper cardstock bridges. The storage bins containing ants and nesting material were then slowly flooded with tap water to stimulate the workers and queens to walk across the paper cardstock bridge and move their brood (eggs, larvae, and pupae) into the new lab nesting bins.

CHC Extraction Ants were directly collected after migration into the lab nesting bins, freeze-killed during at least 1 h at −20 °C (Frigidaire, Charlotte, North Carolina, USA), and stored at 7 °C until further use. For single CHC extractions, ants were placed individually into 2 ml GC screw-cap vials (Agilent Technologies, Santa Clara, California, USA) where they were covered with 100 μl of HPLC grade hexane (Fisher Scientific, Fair Lawn, New Jersey, USA) and swirled for 10 min on a Thermolyne Roto Mix (Marshall Scientific, Hampton, New Hampshire, USA). The hexane extracts where then transferred to a fresh conical 250 μl GC insert (Agilent Technologies, Santa Clara, California, USA), where the hexane was subsequently evaporated under a flow of nitrogen

(Praxair, Inc., Danbury, Connecticut). Then, the dried extract was resuspended in 10 μl of a hexane solution containing 7.5 ng/μl of n-dodecane (EMD Millipore Corp., Billerica, Massachusetts, USA) as an internal standard.

For pooled extracts, 100 ants were extracted with 200 μl of HPLC grade hexane and also swirled for 10 min on the Thermolyne Roto Mix. To further separate the non-polar CHC fraction from polar surface lipids in the more highly concentrated pooled extracts, they were then transferred to a Pasteur pipette plugged with glass wool (Supelco, Sigma-Aldrich, St. Louis, Massachusetts, USA) and filled with ~ 1 in. of silica gel desiccant (Fisher Scientific, Fair Lawn, New Jersey, USA). After washing the plugged Pasteur pipette two times with 1 ml of HPLC grade hexane, the extract was added, and eluted with 200 μl of HPLC grade hexane into a new 2 ml GC screw-cap vial with a fresh 250 μl GC insert. Afterwards, the eluted extract of the pooled sample was evaporated under a flow of nitrogen and resuspended in 10 μl of hexane solution containing 7.5 ng/μl of internal n-dodecane standard, undergoing the same treatment as the individual extracts.

GC-MS Analysis Half of the resuspended CHC extract (5 μl) was injected into a gas chromatograph coupled with a mass selective detector (GC: 7890A; MS: 5975C; Agilent Technologies, Santa Clara, California, USA) operating in electron impact mode. The injection was performed in a split/splitless injector in the splitless mode with a temperature of 250 °C. Separation of compounds was performed on a fused silica capillary column (DB-5MS, 30 m × 0.32 mm × 0.25 μm, Agilent J&W GC columns, Santa Clara, California, USA) with a temperature program starting from 80 °C for 5 min and increasing by 80 °C per min to 200 °C, followed by an increase of 5 °C per min to 325 °C which was held for 3 min. Helium with a constant flow of 1.8 ml per min was used as carrier gas.

Peak area integration and calculation was performed using the data analysis software "Enhanced Chemstation", G1701EA, Version E.02.02 (Agilent Technologies, Santa Clara, California, USA). Peaks were automatically integrated with an initial area reject of 0, an initial peak width of 0.017, and an initial threshold of 13. Shoulder detection was turned off. All automatically integrated peak areas were visually inspected and where necessary corrected by manual integration. CHCs were identified according to their retention indices, diagnostic ions, and mass spectra. Where identifications were not possible or ambiguous due to low quantities in individual CHC extracts, the non-polar fractions of the pooled extracts from 100 ants with the same pattern but enriched CHC quantities were consulted to clarify the diagnostic ion based identifications. However, due to partially poor resolution, co-elution of particular methyl alkanes (Carlson et al. 1998) and ambiguities in certain diagnostic ion pairs (i.e., multiple possible positional isomers with different methyl group positions deducible by the diagnostic ions), some co-eluting CHCs could not unambigously be assigned (see also Sunamura et al. 2009). Therefore, we decided to mainly restrict ourselves to the respective CHC compound classes and chain lengths for simplicity and clarity.

Statistical Analysis All subsequent statistical analyses were performed with the statistics program R (R Core Team 2018) on the absolute CHC quantities (in ng) determined with the internal n-dodecane standard. Since total amounts within the five different CHC classes were largely not normally distributed across all sampled *L. humile* populations (see Supplementary Fig. 1), sequential Mann-Whitney U tests were performed for each respective CHC class for consistency. Originally obtained *P*-values were then corrected for the false-discovery rate due to multiple comparisons by Benjamini-Hochberg corrections (Benjamini and Hochberg 1995).

Average monthly temperature and average monthly precipitation rates for each *L. humile* collection site were obtained from the publicly available repository at http://www.worldclim.org/ through matching with the longitudinal and latitudinal data for each respective collection month and location. Subsequent correlation analyses between the obtained climatic factors and the respective total CHC amounts were performed with Benjamini-Hochberg corrected Spearman rank correlation tests.

To project the high-dimensional data points into two dimensions, the ordination method "**n**onmetric **m**ulti**d**imensional **s**caling" (NMDS) from the R package "vegan" (Oksanen et al. 2007) was used. Reducing the dimensionality with this method, the data points are plotted in a monotonous way so that the calculated distances (δ) in the plot give the most accurate reflection of the actual distances (d) between the data. Two preconditions are met with the NMDS method:

1. The calculated distances in the plot are **smaller or equal** to the actual data point distances ($\delta_{i,j} \leq d_{i,j}$)
2. The correlation between the calculated distances and the actual data point distances is maximized ($cor(\delta_{i,j}, d_{i,j}) \leftrightarrow max$)

Thus, the NMDS method attempts a visual representation of data point distances emphasizing the maintenance of the actual differences in the dataset. A further advantage of this method is its independence from sample-size.

Results

CHC Distribution between Populations The CHC composition of *L. humile* populations consists of five main classes: *n*-alkanes, *n*-alkenes, monomethyl alkanes, dimethyl alkanes, and

trimethyl alkanes (Fig. 2, see also Table 1). Separated into each respective CHC class, the total amounts partially differ among our collected populations, though no discernible colony-, habitat-, or season-specific pattern could be observed. The one collection site that was sampled on three different time points (Sweetwater; SW) displayed changes in CHC composition through time (Fig. 2a, b). Specifically, the sample from SW collected in May showed significantly higher *n*-alkene amounts than both SW samples collected in January (*Mann-Whitney U test*, W = 4, $P < 0.001$) and in April (*Mann-Whitney U test*, W = 13, $P < 0.05$) and significantly higher *n*-alkane amounts than the sample collected in April (*Mann-*

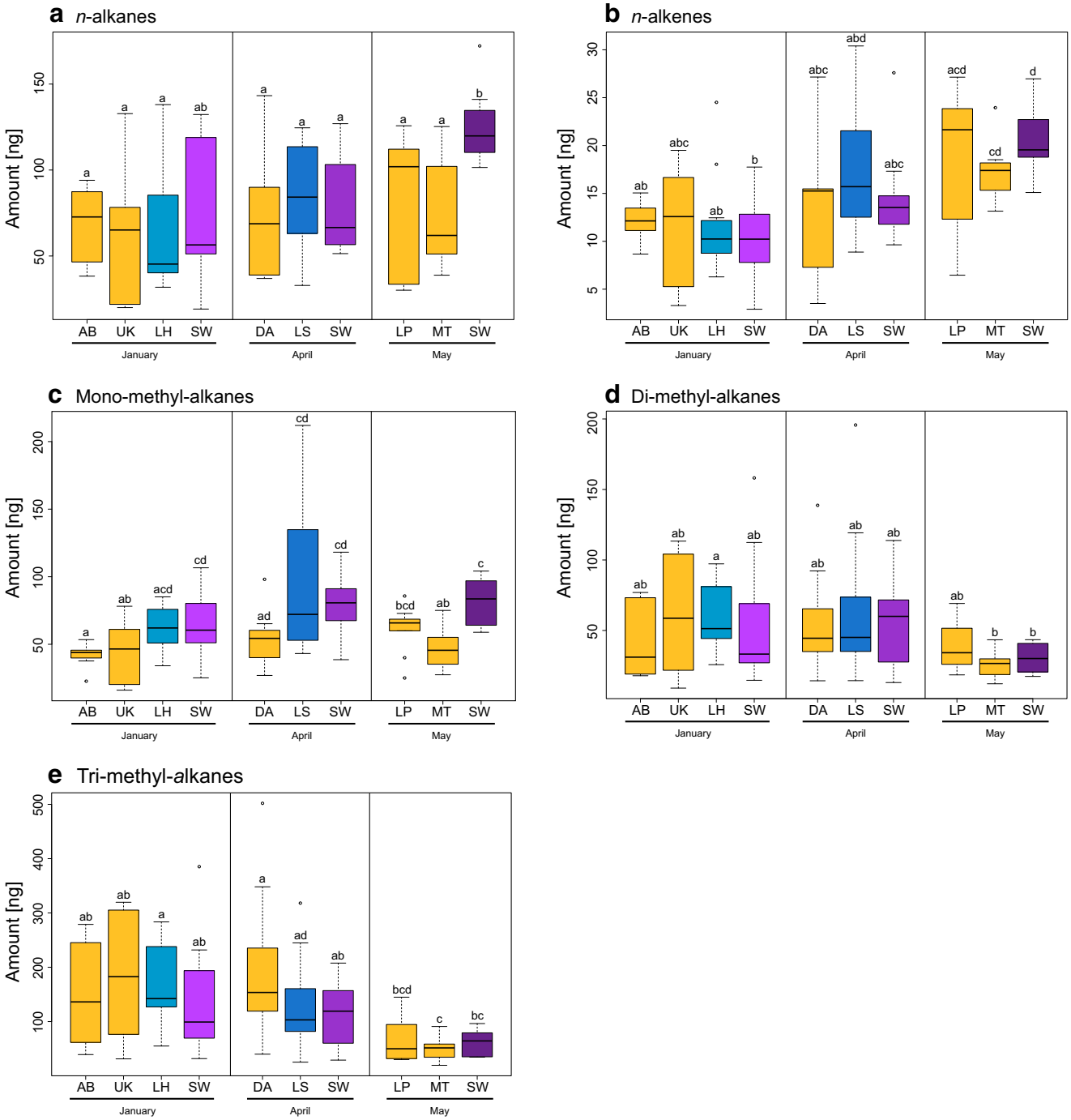

Fig. 2 Total CHC amounts in all of our collected populations of *L. humile* separated by compound classes: **a** *n*-alkanes; **b** *n*-alkenes; **c** Monomethyl alkanes; **d** Dimethyl alkanes; **e** Trimethyl alkanes. Within each compound class, the median of the total CHC amount (ng) was compared between populations with sequential Benjamini-Hochberg corrected Mann-Witney U tests, different letters indicate significant differences among treatment groups. Color shades indicate the affiliation of the respective *L. humile* population to either the main super colony (gold) or the secondary supercolonies (shades of blue and violet)

Table 1 CHC compounds with their respective retention indices (RI), structure assignments, abundances and standard deviations (in ng) identified from all collected *L. humile* populations

RI	Structure assignment	Abundances by *L. humile* population/month (ng ± SD)									
		AB (Jan)	DA (Apr)	LH (Jan)	LP (May)	LS (Apr)	MT (May)	SW (Apr)	SW (Jan)	SW (May)	UK (Jan)
1675	C17:1 n-alkene	0.37 ± 0.11	0.78 ± 0.29	0.4 ± 0.25	0.57 ± 0.28	0.54 ± 0.39	0.49 ± 0.23	0.43 ± 0.34	0.37 ± 0.19	0.66 ± 0.19	0.31 ± 0.24
1700	C17 n-alkane	2.47 ± 1.02	5.35 ± 2.35	4.69 ± 3.56	4.56 ± 2.18	5 ± 4.6	4.84 ± 1.92	3.73 ± 2.96	2.75 ± 1.12	6.3 ± 2.44	2.83 ± 2.45
1760	MeC17 alkane	1.23 ± 0.8	1.34 ± 0.82	0.73 ± 0.66	1.62 ± 1.4	1.75 ± 1.27	1.41 ± 1.48	1.32 ± 0.74	0.98 ± 0.92	2.15 ± 0.68	0.77 ± 0.67
1780	MeC17 alkane	1.78 ± 0.91	1.69 ± 1.2	0.99 ± 0.78	1.84 ± 1.45	1.9 ± 1.02	1.27 ± 1.07	1.29 ± 0.76	1.24 ± 1.17	2.79 ± 0.57	1.11 ± 0.9
1800	C18 n-alkane	1.76 ± 1.17	1.81 ± 1.62	1.08 ± 0.79	1.67 ± 1.28	1.65 ± 0.93	1.23 ± 1	1.38 ± 0.98	1.47 ± 1.32	3.06 ± 0.54	1.65 ± 1.48
1880	C19:1 n-alkene	10.37 ± 1.62	11.39 ± 7.52	10.66 ± 4.57	16.27 ± 6.01	15.29 ± 6.24	15.34 ± 3.09	13.34 ± 4.7	8.76 ± 3.26	17.59 ± 3.51	9.58 ± 5.27
1900	C19 n-alkane	2.97 ± 1.34	4.82 ± 5.05	2.24 ± 1.58	3.48 ± 1.83	3.82 ± 1.5	3.29 ± 1.9	3.66 ± 2.44	4 ± 3.63	6.02 ± 1.17	2.86 ± 2.32
2000	C20 n-alkane	5.59 ± 4.69	4.8 ± 3.61	2.6 ± 2.91	5.48 ± 3.59	4.54 ± 3.3	3.05 ± 2.9	3.39 ± 1.82	3.45 ± 3.55	8.56 ± 2.18	3.98 ± 3.79
2100	C21 n-alkane	6.28 ± 3.69	5.12 ± 3.01	6.45 ± 4.04	6.01 ± 3.53	6.07 ± 3.04	4.83 ± 3	4.81 ± 2.42	7.32 ± 3.26	9.39 ± 1.11	5.53 ± 4.23
2300	C23 n-alkane	9.28 ± 4.3	7.38 ± 4.26	6.27 ± 2.88	9.08 ± 5.66	8.32 ± 3.37	7.46 ± 3.46	7 ± 4.01	8.84 ± 5.02	13.77 ± 2.13	7.96 ± 5.55
2500	C25 n-alkane	6.21 ± 3.26	6.39 ± 5	5.81 ± 3.48	6.83 ± 4.75	8.7 ± 3.6	5.68 ± 3.3	8.73 ± 3.1	8.27 ± 6.61	13.4 ± 2.42	5.09 ± 5.36
2600	C26 n-alkane	3.18 ± 2.44	3.23 ± 2.38	2.45 ± 2.74	4.2 ± 3.02	4.56 ± 2.03	3.73 ± 3.26	4.05 ± 2.05	3.87 ± 3.41	8.29 ± 2.05	2.03 ± 2.58
2700	C27 n-alkane	16.42 ± 3.9	17.32 ± 6.61	18.21 ± 12.7	18.74 ± 8.72	21.93 ± 9.83	19.01 ± 7	23.19 ± 10.84	18.52 ± 8.01	26.84 ± 7.52	13.27 ± 7.06
2731	MeC27 alkanes	1.81 ± 1.7	1.66 ± 1.35	3.1 ± 1.57	3.17 ± 2.22	4.96 ± 4	2.37 ± 1.92	4.41 ± 1.58	3.76 ± 2.66	8.66 ± 2.28	1.64 ± 2.39
2754	MeC27 alkane	1.85 ± 1.28	1.77 ± 1.18	2.16 ± 2.17	2.43 ± 1.97	2.05 ± 1.14	1.54 ± 1.76	1.8 ± 1.4	2.21 ± 1.56	4.17 ± 1.25	1.54 ± 1.51
2777	MeC27 alkane	3.72 ± 1.39	5.07 ± 2.18	5.07 ± 3.17	5.98 ± 3.49	5.78 ± 3.52	4.27 ± 2.17	4.89 ± 1.9	6.59 ± 3.48	6.83 ± 1.9	3.04 ± 1.58
2800	C28 n-alkane	3.02 ± 1.99	3.2 ± 2.01	2.35 ± 1.75	4.66 ± 2.7	3.9 ± 1.65	4.09 ± 2.14	3.93 ± 1.53	3.68 ± 2.58	7.28 ± 1.77	2.65 ± 2.49
2900	C29 n-alkane	6.38 ± 1.9	6.71 ± 3.64	5.97 ± 3.67	10.48 ± 5.15	7.2 ± 2.74	11.12 ± 3.59	9.27 ± 3	6.95 ± 3.55	12.3 ± 2.84	7.84 ± 4.95
2931	MeC29 alkanes	1.68 ± 1.44	1.8 ± 1.44	2.5 ± 1.28	3.1 ± 1.89	5.97 ± 5.14	2.12 ± 1.15	5.87 ± 2.75	3.56 ± 2.09	7.27 ± 1.67	1.32 ± 1.14
2938	C30:1 n-alkene	1.33 ± 0.78	1.08 ± 0.54	0.77 ± 0.79	2.02 ± 1.13	1.27 ± 0.64	1.31 ± 0.79	0.78 ± 0.45	1.32 ± 0.95	2.21 ± 0.41	1.59 ± 1.66
2954	MeC29 alkane	1.22 ± 0.75	1.39 ± 1.09	1.27 ± 1.05	2.23 ± 1.98	1.74 ± 0.65	1.77 ± 1.18	2.53 ± 1.64	1.64 ± 1.4	2.71 ± 1	1.83 ± 1.24
2969	MeC29 alkane	2.02 ± 0.81	2.64 ± 1.52	2.68 ± 1.21	3.25 ± 2.12	3.09 ± 1.62	2.73 ± 1.29	3.09 ± 0.94	3.32 ± 1.62	4.7 ± 0.7	1.99 ± 1.11
2977	DiMeC29 alkane	1.79 ± 0.98	1.84 ± 1.26	2.24 ± 1.82	2.17 ± 2.11	1.58 ± 0.71	1.17 ± 1.15	1.67 ± 0.73	2.06 ± 0.91	3.08 ± 0.87	1.85 ± 1.14
3000	n-C30 (+ MeC30 alkane + DiMeC29 alkanes)	2.18 ± 1.4	1.6 ± 1.13	3.23 ± 1.91	1.98 ± 1.01	3.13 ± 1.33	1.45 ± 1.27	2.95 ± 1.73	2.98 ± 1.77	5.65 ± 1.29	1.91 ± 1.54
3100	C31 n-alkane	1.47 ± 0.8	1.37 ± 0.77	1.35 ± 0.84	2.4 ± 1.15	2.11 ± 0.76	2.21 ± 0.79	1.88 ± 0.69	1.74 ± 0.95	3.02 ± 0.43	1.73 ± 1.56
3125	MeC31 alkane	2.96 ± 1.12	3.89 ± 1.88	5.76 ± 2.26	6.93 ± 2.2	12.33 ± 7.8	4.46 ± 1.33	8.75 ± 3.43	4.16 ± 1.34	8.9 ± 2.31	2.9 ± 2.1
3149	MeC31 alkane	1.32 ± 1.1	2.54 ± 0.71	2.77 ± 1.28	2.82 ± 1.33	7.18 ± 5.04	2.1 ± 1.35	7.64 ± 3.89	3.74 ± 1.65	8.81 ± 2.73	1.26 ± 1.7
3158	DiMeC31 alkanes	0.86 ± 0.64	1.77 ± 0.57	2.95 ± 0.99	2.51 ± 1.66	5.71 ± 6.41	1.32 ± 0.64	4.01 ± 2.74	1.95 ± 1.93	1.18 ± 0.52	0.22 ± 0.33
3167	MeC31 alkane	1.16 ± 0.58	1.31 ± 0.5	1.14 ± 0.65	0.96 ± 0.37	1.01 ± 1.11	1.05 ± 0.59	0.71 ± 0.33	0.6 ± 0.4	0.96 ± 0.24	0.73 ± 0.29
3175	DiMeC31 alkanes	1.56 ± 0.96	2.42 ± 1.27	2.35 ± 1.21	2.07 ± 0.84	2.52 ± 0.96	1.2 ± 0.64	1.99 ± 0.85	1.48 ± 0.57	1.97 ± 0.76	1.93 ± 1.29
3183	TriMeC31 alkane	X	X	4.43 ± 2.11	X	8.94 ± 7.02	0.03 ± 0.1	7.02 ± 3.25	5.49 ± 2.52	6.16 ± 3.18	X
3192	TriMeC31 alkanes	X	X	10.19 ± 3.61	X	12.27 ± 8.66	0.06 ± 0.19	9.28 ± 3.67	8.98 ± 4.23	7.21 ± 3.09	X
3200	TriMeC31 alkanes (+ DiMeC31 alkane)	6.22 ± 2.33	8.37 ± 4.19	14.56 ± 5.28	4.51 ± 1.69	11.26 ± 6.06	2.71 ± 1.49	8.63 ± 3.24	11.47 ± 5.19	8.59 ± 3.13	6.09 ± 3.18

Table 1 (continued)

RI	Structure assignment	Abundances by *L. humile* population/month (ng ± SD)									
		AB (Jan)	DA (Apr)	LH (Jan)	LP (May)	LS (Apr)	MT (May)	SW (Apr)	SW (Jan)	SW (May)	UK (Jan)
3225	TriMeC31 alkanes	2.67 ± 1.05	4.07 ± 1.65	9.49 ± 3.54	3.12 ± 1.43	9.58 ± 4.99	1.78 ± 1.21	5.88 ± 2.14	6.93 ± 2.47	5.62 ± 1.48	2.49 ± 1.71
3258	MeC32 alkane	0.56 ± 0.34	1.16 ± 0.65	2.96 ± 1.01	1.09 ± 0.7	3.34 ± 2.63	0.35 ± 0.39	2.3 ± 1.02	2.79 ± 1.37	2.45 ± 0.79	0.7 ± 0.88
3283	DiMeC32 alkanes	1.03 ± 0.33	1.29 ± 0.66	2.09 ± 0.69	0.74 ± 0.43	2.42 ± 1.43	0.36 ± 0.27	1.87 ± 0.79	2.19 ± 1.01	1.78 ± 0.57	0.92 ± 0.54
3300	C33 n-alkane	0.88 ± 0.19	0.86 ± 0.44	2.17 ± 0.82	1.05 ± 0.58	1.84 ± 0.98	0.78 ± 0.21	1.22 ± 0.4	1.6 ± 0.76	1.27 ± 0.32	1.02 ± 0.59
3309	DiMeC33 alkane	2.37 ± 1.04	2.08 ± 0.9	3.04 ± 1.7	2.86 ± 1.32	4.46 ± 2.89	2.16 ± 0.71	3.6 ± 1.8	2.36 ± 1.57	2.79 ± 1.14	1.36 ± 0.77
3327	MeC33 alkanes	2.09 ± 0.82	2.87 ± 1.24	8.76 ± 3.09	5.68 ± 1.36	14.97 ± 10.15	4.09 ± 1.07	8.69 ± 3.82	7.03 ± 3.72	6.94 ± 2.74	2.91 ± 1.82
3345	MeC33 alkane + DiMeC33 alkane	1.86 ± 1.03	2.33 ± 1.2	4.28 ± 1.4	2.46 ± 0.9	8.45 ± 6.33	1.61 ± 0.43	5.74 ± 2.5	5.22 ± 2.65	4.25 ± 1.8	2.17 ± 1.56
3355	DiMeC33 alkanes	X	X	4.06 ± 1.97	1.59 ± 0.77	5.1 ± 3.46	0.91 ± 0.46	4.22 ± 2.06	3.27 ± 1.99	2.88 ± 1.19	0.17 ± 0.33
3373	MeC33 alkane + DiMeC33 alkanes	7.25 ± 4.03	9 ± 4.88	6.6 ± 2.73	6.64 ± 2.32	7.89 ± 4.06	4.57 ± 1.26	5.7 ± 2.45	4.78 ± 3.79	3.85 ± 1.61	7.97 ± 5.71
3382	DiMeC33 alkanes	X	X	8.6 ± 3.96	X	11.13 ± 8.06	0.14 ± 0.46	10.85 ± 4.39	10.98 ± 6.33	7.29 ± 3.24	X
3391	TriMeC33 alkanes	X	X	12.62 ± 5.49	X	8.7 ± 6.63	0.25 ± 0.8	6.8 ± 2.96	7.05 ± 4.29	3.88 ± 1.63	X
3400	TriMeC33 alkanes (+ DiMeC33 alkanes)	22.53 ± 13.38	26.81 ± 15.67	23.33 ± 9.64	11.08 ± 4.83	15.36 ± 9.6	7.87 ± 2.06	10.9 ± 5.34	14.03 ± 9.01	6.9 ± 2.76	25.39 ± 16.6
3409	TriMeC34 alkane	X	X	7.9 ± 4.8	X	2.85 ± 2.63	0.25 ± 0.8	2.38 ± 1.32	3.6 ± 2.69	1.17 ± 0.83	X
3427	TriMeC34 alkanes	5.44 ± 3.52	6.05 ± 4.03	10.92 ± 4.94	2.69 ± 1.27	6.25 ± 4.88	1.92 ± 0.78	4.56 ± 2.37	6.17 ± 4.4	2.59 ± 1.07	5.7 ± 4.06
3455	DiMeC34 alkanes	1.7 ± 1.37	1.26 ± 1.01	4.12 ± 2.49	0.39 ± 0.26	1.62 ± 2.77	0.27 ± 0.35	1.82 ± 1.46	2.24 ± 2.32	0.21 ± 0.28	1.96 ± 1.98
3482	DiMeC34 alkanes (+ TriMeC34 alkane)	1.17 ± 0.88	1.48 ± 1.13	2.61 ± 1.68	0.59 ± 0.71	1.65 ± 1.66	0.28 ± 0.27	1.54 ± 1.09	1.86 ± 1.84	0.53 ± 0.29	1.57 ± 1.53
3491	DiMeC34 alkanes	1.28 ± 0.99	1.65 ± 1.35	2.28 ± 1.49	0.34 ± 0.45	1.14 ± 1.24	0.16 ± 0.23	0.6 ± 0.5	1.07 ± 1.61	0.27 ± 0.17	1.87 ± 1.34
3491	MeC34 alkanes	1.92 ± 1.27	2.21 ± 1.44	0.15 ± 0.19	1.1 ± 0.75	0.69 ± 1.1	0.97 ± 0.29	0.56 ± 0.5	0.71 ± 1.21	0.22 ± 0.16	2.14 ± 1.33
3509	TriMeC34 alkane	4.75 ± 3.33	5.92 ± 4.31	3.23 ± 1.73	1.15 ± 1.06	0.99 ± 0.89	0.75 ± 0.46	1 ± 0.91	1.86 ± 1.98	0.37 ± 0.21	4.67 ± 3.37
3527	MeC35 alkane	4.08 ± 2.53	5.24 ± 3.5	7.3 ± 4.01	5.83 ± 2.09	10.01 ± 8.06	5.34 ± 2.1	7.42 ± 4.21	6.55 ± 5.15	3.78 ± 1.65	5.9 ± 4.41
3545	DiMeC35 alkanes	4.79 ± 3.47	6.26 ± 4.61	9.54 ± 5.41	5.41 ± 2.82	11.66 ± 10.85	3.9 ± 2.09	9.16 ± 5.79	9.21 ± 8.22	4.24 ± 1.97	7.71 ± 5.64
3575	DiMeC35 alkanes	13.81 ± 9.76	16.23 ± 11.73	0.33 ± 1.1	10.04 ± 5.49	X	7.28 ± 2.52	X	X	X	16.65 ± 11.65
3578	TriMeC35 alkane	X	X	14.91 ± 9.39	0.2 ± 0.62	13.01 ± 10.18	0.57 ± 1.81	13.71 ± 7.96	14.35 ± 12.44	5.38 ± 2.41	X
3591	TriMeC35 alkanes	X	X	6.58 ± 4.41	X	3.55 ± 3.36	X	3.37 ± 2.57	3.92 ± 3.58	1.28 ± 0.55	X
3600	TriMeC35 alkanes (+ DiMeC35 alkane)	60.27 ± 41.65	75.37 ± 54.4	24.51 ± 14.59	21.68 ± 13.88	18.14 ± 13.97	17.7 ± 7.63	17.19 ± 12.06	22.97 ± 21.5	5.91 ± 2.78	67.9 ± 44.86
3620	TriMeC35 alkanes	10.97 ± 10.2	17.47 ± 13.8	7.64 ± 5.25	4.25 ± 3.45	4.66 ± 4.36	3.4 ± 1.8	4.32 ± 3.49	6.21 ± 6.84	1.15 ± 0.58	14.69 ± 10.25
3650	DiMeC36 alkanes	2.43 ± 1.97	3.43 ± 2.79	2.78 ± 2.58	1.43 ± 1.82	1.96 ± 2.77	0.78 ± 0.84	1.72 ± 1.93	2.62 ± 3.9	0.4 ± 0.25	5.45 ± 6.62
3690	TriMeC36 alkanes	4.43 ± 3.78	4.54 ± 3.22	2.49 ± 2.07	1.1 ± 1.8	0.71 ± 1.27	0.57 ± 0.34	1.24 ± 1.45	1.7 ± 2.24	0.06 ± 0.06	5.91 ± 4.92
3697	TriMeC36 alkane	4.3 ± 3.64	6.1 ± 5.3	1.07 ± 1.35	0.86 ± 1.27	0.59 ± 0.82	0.56 ± 0.45	0.8 ± 0.92	1.55 ± 2.1	0.06 ± 0.06	4.84 ± 3.78
3727	MeC37 alkanes	3.14 ± 2.38	4.59 ± 4.29	2.72 ± 2.12	2.91 ± 1.89	4.11 ± 4.12	3.18 ± 1.93	3.71 ± 3	3.6 ± 4.33	1.15 ± 0.47	4.14 ± 3.53
3745	DiMeC37 alkanes	6 ± 4.94	9.11 ± 7.56	8.03 ± 6.66	4.39 ± 3.38	9.37 ± 12.27	3.63 ± 2.05	8.59 ± 7.05	9.1 ± 10.46	2.18 ± 0.99	9.88 ± 7.87
3764	DiMeC37 alkanes	1.71 ± 1.92	2 ± 1.73	0.23 ± 0.28	1.01 ± 0.76	0.62 ± 0.77	0.64 ± 0.4	0.58 ± 0.88	1.16 ± 1.39	0.29 ± 0.15	3.37 ± 2.75
3773	TriMeC37 alkane + DiMeC37 alkanes	5.25 ± 4.57	7.66 ± 6.65	6.09 ± 6.01	3.86 ± 2.93	3.76 ± 3.86	3.72 ± 2.55	5.26 ± 4.46	5.39 ± 6.54	1.11 ± 0.54	9.4 ± 7.98
3782	TriMeC37 alkanes	1.09 ± 1.08	1.62 ± 1.36	2.04 ± 2.09	0.5 ± 0.46	1.83 ± 2.08	0.19 ± 0.26	2.6 ± 2.82	3.68 ± 4.17	0.66 ± 0.31	0.83 ± 0.91

Table 1 (continued)

RI	Structure assignment	Abundances by *L. humile* population/month (ng ± SD)									
		AB (Jan)	DA (Apr)	LH (Jan)	LP (May)	LS (Apr)	MT (May)	SW (Apr)	SW (Jan)	SW (May)	UK (Jan)
3800	TriMeC37 alkanes (+ DiMeC37 alkanes)	18.37 ± 16.5	29.63 ± 25.52	6.69 ± 6.21	7.43 ± 6.66	5.45 ± 5.41	5.88 ± 3.5	6.45 ± 5.88	9.46 ± 12.12	1.37 ± 0.71	26.33 ± 21.59
3822	TriMeC37 alkanes	5.78 ± 5.57	9.85 ± 9.03	2.58 ± 2.43	1.49 ± 1.64	1.68 ± 1.95	1.33 ± 0.91	1.95 ± 2.27	3.26 ± 4.4	0.37 ± 0.28	7.33 ± 6.11
3844	DiMeC38 alkanes	1.93 ± 2.32	3.53 ± 3.22	1.49 ± 1.6	0.73 ± 0.86	0.89 ± 1.38	0.35 ± 0.32	1.18 ± 1.24	1.77 ± 2.06	0.21 ± 0.22	3.14 ± 3.08
3927	MeC39 alkanes	0.75 ± 0.64	1.56 ± 1.38	1.06 ± 0.61	1.24 ± 0.58	1.04 ± 0.64	1.08 ± 0.66	1.66 ± 1.48	1.42 ± 1.06	0.83 ± 0.64	1.31 ± 1.18
3945	DiMeC39 alkanes	1.6 ± 2.03	3.07 ± 2.74	2.35 ± 2.09	1.36 ± 0.95	1.79 ± 2.2	0.93 ± 0.78	1.96 ± 1.91	2.43 ± 2.77	0.61 ± 0.49	2.51 ± 2.47

Chain lengths and the respective CHC compound classes are given. X indicates non-detectable amounts of the respective compound. Compounds in parentheses indicate trace amounts detected in addition to the predominant compound

Whitney U test, W = 11, $P < 0.01$). The five samples from the main California supercolony were not significantly different for total amount of *n*-alkanes or dimethyl alkanes regardless of collection month and site (Fig. 2a), whereas the other three CHC classes (*n*-alkenes, mono-, and trimethyl alkanes) did, indeed, show significantly different amounts across the sampled populations (Fig. 2b–e). Comparing the secondary supercolonies (LH, LS and SW), significant differences emerge for all but monomethyl alkanes, although this particular CHC class still showed high variation within the LS population (Fig. 2c).

Correlations between Climate Factors and CHC Classes We tested for correlations between total amounts of each CHC class and two environmental factors closely associated with desiccation: Average temperature and average precipitation during month of collection (Fig. 3). We found that the total amount of *n*-alkanes and *n*-alkenes were both positively correlated with average monthly temperature (*Spearman rank correlation*, *n*-alkanes: $\rho = 0.78$, $P = 0.01$; *n*-alkenes: $\rho = 0.91$, $P < 0.01$) but negatively correlated with monthly precipitation rates (*Spearman rank correlation*, *n*-alkanes: $\rho = -0.81$, $P = 0.01$; alkenes: $\rho = -0.9$, $P < 0.01$, Fig. 3a, b). Trimethyl alkanes, on the other hand, showed the reversed pattern: The total amount of this CHC class was negatively correlated with average monthly temperature (*Spearman rank correlation*, $\rho = -0.85$, $P < 0.01$), but positively correlated with monthly precipitation rates (*Spearman rank correlation*, $\rho = 0.86$, $P < 0.01$, Fig. 3c). It should be noted that individually identified CHCs assigned to the latter CHC class partially also contained traces of dimethyl alkanes (see Table 1). Thus, dimethyl alkanes, despite not correlating as a separate CHC class with temperature and precipitation, cannot be ruled out completely in their contribution to the correlation found together with trimethyl alkanes.

Correlations between Climate Factors and Individual CHCs For each CHC class that was correlated with average monthly temperature and precipitation (i.e., *n*-alkanes, *n*-alkenes, and trimethyl alkanes), we plotted the individual CHCs simulaneously into two chromatograms obtained from pooled non-polar fractions from one main (AB) and one secondary (LS) supercolony collection site (Fig. 4). In total, two *n*-alkenes were positively correlated with average monthly temperature and negatively with average monthly precipitation, with chain lengths of 17 and 19 carbons, respectively, whereas the five *n*-alkanes with these same correlations had carbon chain lengths from 27 to 31. All trimethyl alkanes (as well as the co-eluting traces of dimethyl alkanes), which showed reverse correlations (see Fig. 3), had longer carbon chains ranging from 33 to 37. Thus, all of the correlating methylbranched CHCs were found at the end of the detectable spectrum of compounds and possessed the highest number of

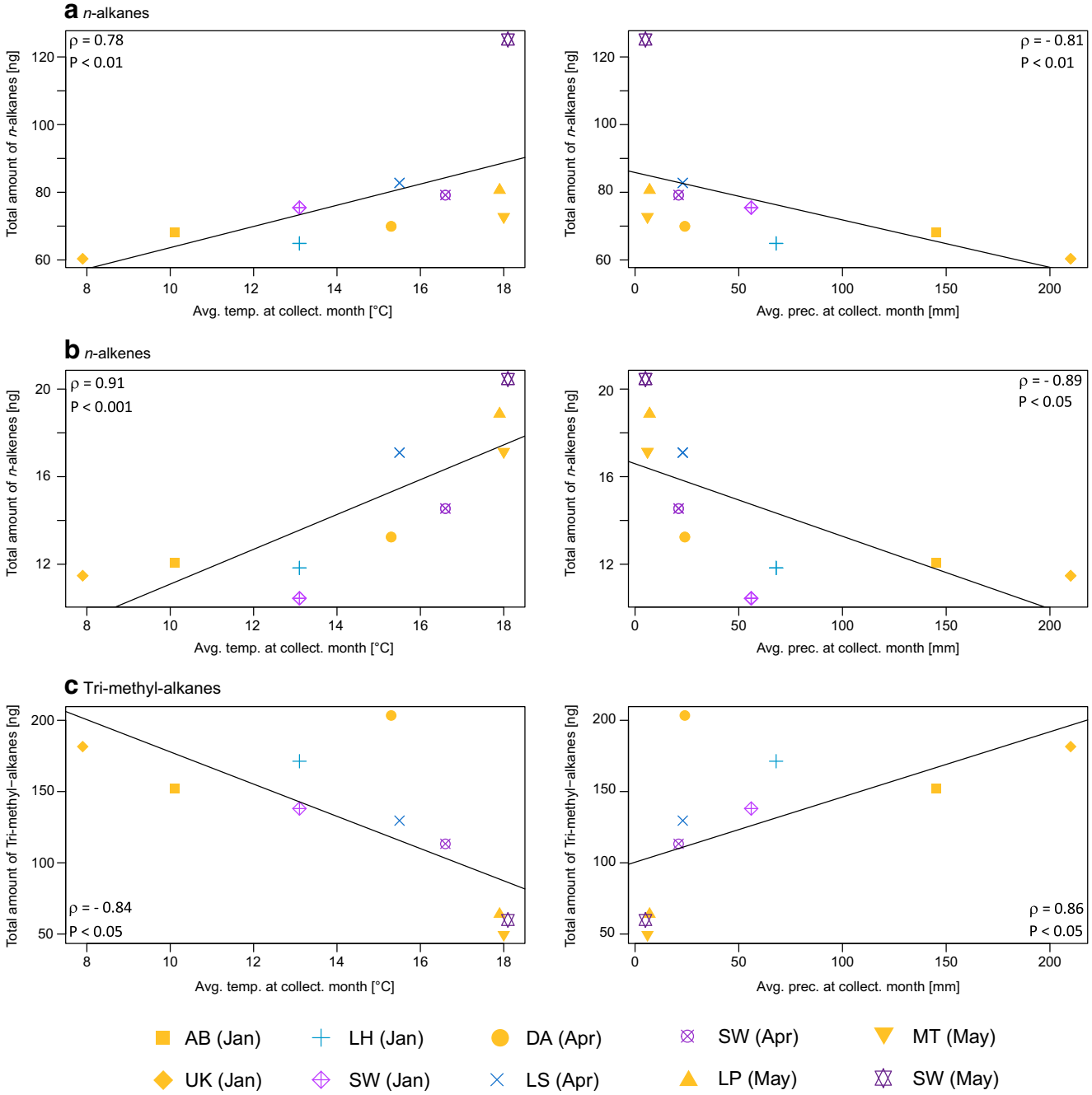

Fig. 3 Significant correlations between total CHC amounts and average temperature (in °C, left) as well as average precipitation (in mm, right) per month and collection location for our *L. humile* populations, separated by CHC class:A) n-alkanes; B) n-alkenes; C) trimethyl alkanes. Different *L. humile* populations are represented by different symbols, with color shades indicating their affiliation to either the main supercolony (gold) or the secondary super colonies (shades of blue and violet). Significance in the correlations was assessed through Benjamini-Hochberg corrected Spearman rank correlations tests, resulting test statistics (ρ and *P* value) are indicated in the respective plots

carbons (Fig. 4). Correlation plots and the respective test statistics for all correlated individual CHCs are given in Supplementary Fig. 2 and Supplementary Table 1, respectively.

Total CHC Variation and Colony Divergence When we visualized the total CHC variation, including all compounds regardless of their correlations with environmental factors, the *L. humile* populations clearly clustered into two groups reflecting their respective colony affiliation (Fig. 5). The ants from the main supercolony were separated from the various secondary supercolonies when total CHC divergence was taken into account, irrespective of collection month and site (see also Fig. 1). It is interesting to note that while all SW samples

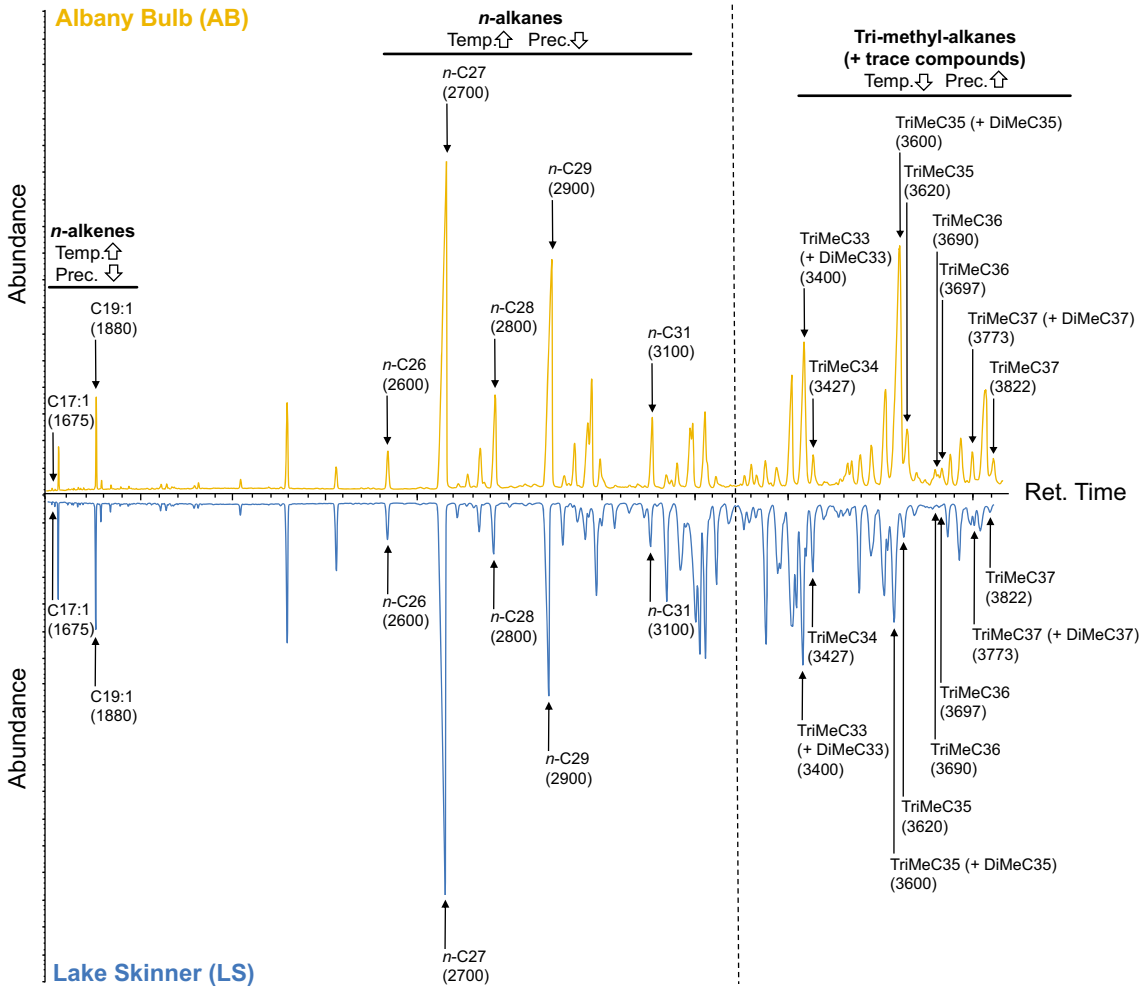

Fig. 4 CHC profiles of representative *L. humile* populations for the main super colony (AB, gold, above) and secondary super colonies (LS, blue, below), mirrored for comparison. For clarity, each individual CHC significantly correlating with both average monthly temperature and precipitation levels is labeled with a compound ID and the respective retention index in parentheses (compare to Table 1). They are further summarized according to their corresponding compound classes, with their respective correlation with average monthly temperature (temp.) and precipitation levels (prec.) indicated by arrows (upwards arrow: positive correlation, downwards arrow: negative correlation). The chromatograms were generated with non-polar fractions of pools of 100 individuals per collected population. For the corresponding correlation graphs and test statistics of each of the individual CHCs see Supplementary Fig. 2 and Supplementary Table 1

generally clustered together with the other secondary supercolonies, the seasonal variation was still reflected in the slight divergence between all three SW samples collected in different months, most notably for the sample collected in May (compare to Fig. 2).

Discussion

Although CHCs are known to play a central role in insect desiccation resistance, specific contributions of particular CHC classes or individual CHCs are rarely assessed (Chung and Carroll 2015; Menzel et al. 2017). To identify candidate CHCs for desiccation resistance, we examined CHC profiles of the invasive Argentine ant, *Linepithema humile*, across a variety of geographically distant sites in northern and southern California (Fig. 1). Focusing on two climatic factors closely associated with humidity and desiccation, i.e., temperature and precipitation, we found interesting reciprocal correlations with a subset of CHCs classes identified from our various *L. humile* populations. The total amounts of *n*-alkanes and *n*-alkenes were positively correlated with monthly average temperature, but negatively with monthly average precipitation (Fig. 3). This indicates their potential to be functionally recruited for waterproofing and desiccation resistance, a trait found to be closely associated with *n*-alkanes in several studies, but much less with *n*-alkenes so far (e.g., Gibbs and Rajpurohit 2010; Wagner et al. 2001). However, despite intermediate melting temperatures and volatility of *n*-alkenes as opposed to the superior waterproofing properties of *n*-alkanes, it has recently been suggested that *n*-alkenes could directly influence desiccation resistance as well (Chung and Carroll

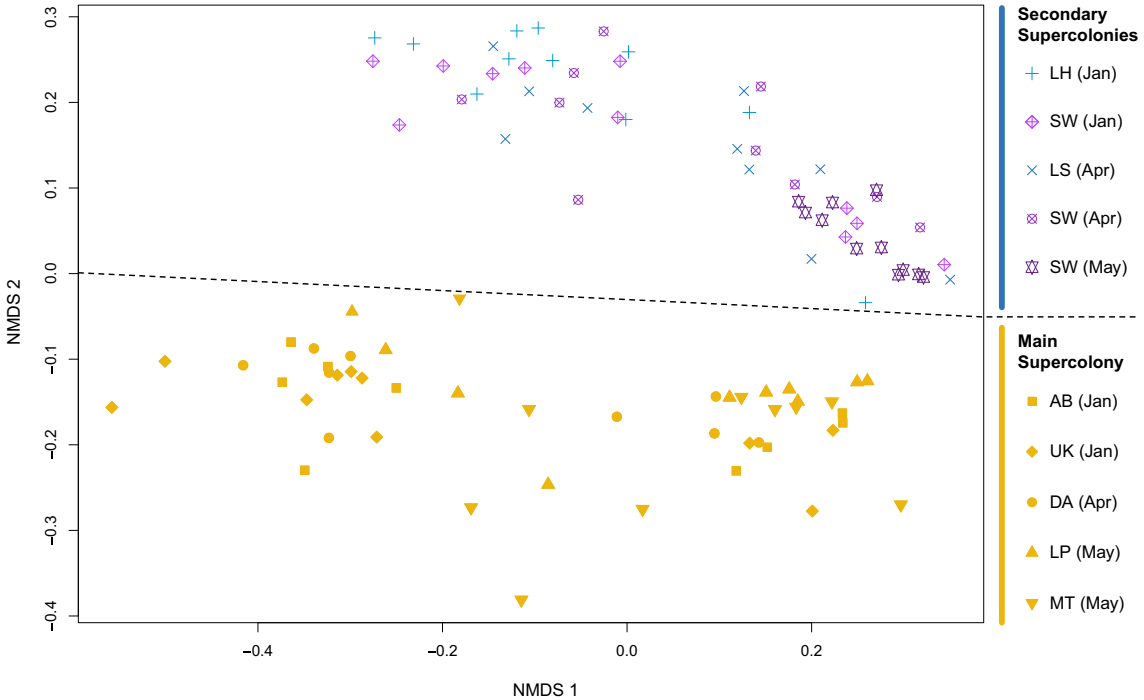

Fig. 5 Non-metric multidimensional scaling (NMDS) plot representing all CHC differences between individual worker extracts of our collected *L. humile* populations. Bray-Curtis distances were used to calculate the divergence of the populations based on their CHC differences. A dotted line represents the separation of the different *L. humile* populations according to their colony affiliation, which is further indicated by their color schemes (main super colony: gold, secondary super colonies: blue/violet shadings)

2015; Ferveur et al. 2018). Trimethyl alkanes, on the other hand, showed the reverse correlation, being negatively correlated with monthly average temperature, but positively with monthly average precipitation (Fig. 3). This suggests that this compound class is generally less important for desiccation resistance, which has been hypothesized for a long time due to their physiological properties being less suited for water-proofing (Chung and Carroll 2015; Gibbs and Pomonis 1995; Gibbs and Rajpurohit 2010;). This might also indicate a higher degree of flexibility for this compound class to be used in other functions, e.g., signaling, as the selective constraints to be recruited for dessication resistance seem less strong. This is in accordance with studies reporting that due to their higher potential for coding information, CHCs with several methyl branches comprise main signaling components in CHC profiles, while generally being less important for water-proofing (Blomquist and Bagnères 2010; Howard and Blomquist 2005). However, empirical studies using isolated methyl-branched CHCs as the sole conveyors of chemical information are still relatively scarce (e.g., Brandt et al. 2009; Krasnec and Breed 2013; Sakata et al. 2017).

Studies on the influence of environmental factors on CHC profiles in other ant taxa yielded partially similar, but also quite divergent correlations from those found in our study. For instance, a survey encompassing 38 acrobat ant species (genus *Crematogaster*) and 42 carpenter ant species (genus *Camponotus*) found no correlations between mean annual temperature and CHC quantities (Menzel et al. 2017). By using average monthly temperatures matching the respective collection months rather than annual mean temperature, we were able to reveal temperature correlations with several CHC classes (see above), indicating high sensitivity to temperature and seasonality in *L. humile* CHC profiles. Furthermore, the proportion of *n*-alkenes in the studied *Crematogaster* and *Camponotus* species was found to be positively correlated with precipitation rates, a correlation apparently reversed in *L. humile* (see Fig. 3). However, it should be noted that *n*-alkenes occur in the lowest quantities in the *L. humile* CHC profiles compared to all other CHC classes (Fig. 2, see also profile comparison in Fig. 4). Interestingly, *n*-alkenes only occur in the absence of dimethyl alkanes in the studied *Crematogaster* and *Camponotus* species, hinting at partially different biosynthetic mechanisms governing CHC variation in these two genera as opposed to *L. humile*, where the two compound classes do co-occur. In another study on two species of the ant genus *Temnothorax*, portions of *n*-alkanes have been found to be increased in drought conditions, whereas portions of di- and trimethyl alkanes are decreased (Menzel et al. 2018). This partially parallels our results for *L. humile*, as precipitation rates constitute a close approximation to the degree of drought in certain habitats. Also, Wagner et al. (2001) reported that the red harvester ant *Pogonomyrmex barbatus* has the same response as *L. humile* in terms of *n*-alkanes, which are increased in conditions of low humidity and high temperature.

Even in more distantly related insect taxa, interesting similarities to our findings have been discovered, implying more general effects of climatic factors on CHC compositions conserved over larger phylogenetic boundaries. For instance, in three social wasp species of the subfamily Polistinae, temperature was also positively correlated with relative amounts of *n*-alkanes, but negatively with relative amounts of methyl alkanes (Michelutti et al. 2018). Even more distantly related and beyond the Hymenoptera, the West Indian drywood termite, *Cryptotermes brevis*, exhibits very different CHC profiles than *L. humile*, with *n*-alkenes constituting the most prevalent compound class as opposed to the least prevalent one in our study (Woodrow et al. 2000, see Fig. 2). Nevertheless, similar correlative effects with environmental factors have been found, with the total amount of *n*-alkenes showing a positive correlation with temperature and *n*-alkanes showing a negative correlation with humidity (Woodrow et al. 2000). Moreover, it has recently been demonstrated in *Drosophila* fruit flies that increased proportions of *n*-alkenes and alkadienes are linked to increased resistance to desiccation, hinting at similar adaptive mechanisms for n-alkenes as in *L. humile,* allowing for acclimatization to related climatic conditions (Ferveur et al. 2018).

Although the degree of phenotypic plasticity of CHC profiles appears to be highly variable and species-dependent (e.g., Ingleby 2015; Liu et al. 2001; Nielsen et al. 1999), several intriguing case studies clearly showed individual adaptability of CHC profiles to environmental conditions, sometimes on a timescale of weeks (e.g., Gefen et al. 2015; Rajpurohit et al. 2017; Rouault et al. 2004; Wagner et al. 2001). This raises the interesting question about the capabilty of *L. humile* to actively adjust their CHC profiles according to the climatic conditions they encounter, which should be adressed in future studies. In fact, results from our study suggest that some of the identified CHC classes in certain *L. humile* populations have the capability to vary seasonally. The Sweetwater (SW) population was sampled in the same months as all the other studied *L. humile* populations (i.e., January, April and May) to control for seasonal variation (see Fig. 1). Surprisingly, we found a high degree of variation, particularly when comparing total amounts of *n*-alkanes and *n*-alkenes, for the SW samples at the three different time points (Fig. 2), clearly suggesting a potential seasonal effect. Although our study was not designed to test this, it would be useful for future studies to directly address phenotypic plasticity and seasonal variation of CHC profiles in *L. humile*. However, we did not find a consistent seasonal effect when separating CHC variation by compound class. The two populations from the main supercolony (LP and MT) sampled at the same time point and in close proximity to SW (see Fig. 1) only partially showed congruence in total amounts of CHCs with the latter, secondary supercolony, with amounts of *n*-alkanes and monomethyl alkanes being the most divergent compound classes (Fig. 2). Similarly, sample location and colony affiliation did not yield any consistent pattern with total amounts for all five identified CHC classes. However, when plotting CHC variation as a whole, the divergence into main supercolony and secondary supercolonies became very apparent (Fig. 5). This is in accordance with other studies showing that information on species and colony affiliation is coded in the whole collective complexity of CHC profiles rather than in single CHCs or classes (e.g., Buckner et al. 2009; Greene and Gordon 2007).

Regardless of CHC profile adaptability to different environmental conditions, it has been suggested that rainfall in general greatly facilitated the invasion of *L. humile* into new habitats (Heller et al. 2008; Holway et al. 2002), and that proximity to human urban structures, particularly water reserves, appears to have played a major role in their invasive success as well (Gordon and Heller 2014). These factors should also be accounted for in future studies and added to the plethora of potential causes and influences on the tremendous invasive success of *L. humile*. In general, it is difficult to discriminate whether environmental factors have actually shaped CHC profile variation or whether organisms have actively occupied micro-environments according to the already present physiological properties of their CHC profiles. It should also be noted that desiccation resistance is a complex phenotype, likely driven by multiple factors, and it would be useful for future studies to include variables such as body size, food availability, or habitat structure in different populations of *L. humile* supercolonies to achieve a more holistic view on the causes of adaptation to such a vast array of micro-climates.

In conclusion, we found converse correlations between a subset of the CHC classes identified in different *L. humile* populations across California and two climatic factors closely associated with humidity and desiccation. *n*-Alkanes and *n*-alkenes were positively correlated with average monthly temperature but correlated negatively with average monthly precipitation, whereas these correlations were reversed for trimethyl alkanes. These findings point to different functional recruitments for these compound classes. *n*-Alkanes and *n*-alkenes potentially play a more important role in dessication prevention as their total amounts increase in hotter and less humid environments. The total amount of trimethyl alkanes, on the other hand, is reduced in environments with higher desiccation stress, potentially indicating that their presence in the CHC profile plays a different role than desiccation resistance, with signaling being a likely and widely hypothesized candidate. Interestingly, although we did not find any consistent colony-, habitat- or season-specific pattern for separated CHC classes alone, colony-specific signatures (main vs. secondary supercolonies) clearly prevail when the total CHC profile variation is taken into account. However, we found hints of phenotypic plasticity and seasonality potentially affecting CHC profile variation in *L. humile* as well. These should be taken into account in future studies to broaden our

understanding on the potential hierachy and synergy of different factors driving CHC profile divergence.

Acknowledgements This work was supported by the US National Science Foundation (IOS-1557934/1557961), USDA National Institute of Food and Agriculture (2016-67013-24749), USDA Hatch Project (CA-B-INS-0087-H), and the UC Berkeley Bakar Fellows program. Furthermore, the authors would like to thank Thomas Schmitt for his valuable help in CHC identification, Katelyn Sanko and Naomichi Yamamoto for assistance in data analysis, Maria A Tonione for support with obtaining, integrating and analyzing climatic data, Mareike Koppik and Maik Bartelheimer for helpful discussions and assistance in statistical analysis and data representation, two anonymous reviewers for their valuable suggestions and input on the first draft of the manuscript, and Wittko Francke for editing the final version of the manuscript.

Compliance with Ethical Standards

Disclosure of Potential Conflicts of Interest The authors declare that they have no competing interests.

Research Involving Human Participants and/or Animals There is no ethics committee overseeing experimental research on Argentine Ants. However, all efforts were made to treat the animals as humanely as possible.

Informed Consent Not applicable.

References

Benjamini Y, Hochberg Y (1995) Controlling the false discovery rate: a practical and powerful approach to multiple testing. J Royal Stat Soc 57:289–300

Blomquist GJ, Bagnères AG (2010) Insect hydrocarbons: biology, biochemistry, and chemical ecology. Cambridge University Press, New York

Blomquist GJ, Nelson DR, Derenobales M (1987) Chemistry, biochemistry, and physiology of insect cuticular lipids. Arch Insect Biochem Physiol 6:227–265

Brandt M, van Wilgenburg E, Sulc R, Shea KJ, Tsutsui ND (2009) The scent of supercolonies: the discovery, synthesis and behavioural verification of ant colony recognition cues. BMC Biol 7:71. https://doi.org/10.1186/1741-7007-7-71

Buckner JS, Pitts-Singer TL, Guedot C, Hagen MM, Fatland CL, Kemp WP (2009) Cuticular lipids of female solitary bees, *Osmia lignaria* say and *Megachile rotundata* (F.) (Hymenoptera: Megachilidae). Comp Biochem Physiol B: Biochem Mol Biol 153:200–205

Burger R, Lynch M (1995) Evolution and extinction in a changing environment - a quantitative-genetic analysis. Evolution 49:151–163. https://doi.org/10.2307/2410301

Carlson DA, Bernier UR, Sutton BD (1998) Elution patterns from capillary GC for methyl-branched alkanes. J Chem Ecol 24:1845–1865

Chown SL, Sorensen JG, Terblanche JS (2011) Water loss in insects: an environmental change perspective. J Insect Physiol 57:1070–1084. https://doi.org/10.1016/j.jinsphys.2011.05.004

Chung H, Carroll SB (2015) Wax, sex and the origin of species: dual roles of insect cuticular hydrocarbons in adaptation and mating. Bioessays 37:822–830. https://doi.org/10.1002/bies.201500014

Clavero M, García-Berthou E (2005) Invasive species are a leading cause of animal extinctions. Trends Ecol Evol 20:110. https://doi.org/10.1016/j.tree.2005.01.003

Ferveur JF, Cortot J, Rihani K, Cobb M, Everaerts C (2018) Desiccation resistance: effect of cuticular hydrocarbons and water content in *Drosophila melanogaster* adults. Peerj 6:e4318. https://doi.org/10.7717/peerj.4318

Gefen E, Talal S, Brendzel O, Dror A, Fishman A (2015) Variation in quantity and composition of cuticular hydrocarbons in the scorpion *Buthus occitanus* (Buthidae) in response to acute exposure to desiccation stress. Comp Biochem Physiol A Mol Integr Physiol 182:58–63. https://doi.org/10.1016/j.cbpa.2014.12.004

Gibbs A (1995) Physical properties of insect cuticular hydrocarbons: model mixtures and lipid interactions. Comp Biochem Physiol B: Biochem Mol Biol 112:667–672

Gibbs AG (1998) Water-proofing properties of cuticular lipids. Am Zool 38:471–482

Gibbs AG (2002) Lipid melting and cuticular permeability: new insights into an old problem. J Insect Physiol 48:391–400. https://doi.org/10.1016/S0022-1910(02)00059-8

Gibbs A, Pomonis JG (1995) Physical properties of insect cuticular hydrocarbons: the effects of chain-length, methyl-branching and unsaturation. Comp Biochem Physiol B: Biochem Mol Biol 112:243–249

Gibbs AG, Rajpurohit S (2010) Cuticular lipids and water balance. In: Blomquist GJ, Bagnères A-G (eds) Insect hydrocarbons: biology, biochemistry, and chemical ecology. Cambridge University Press, Cambridge, pp 100–120. https://doi.org/10.1017/CBO9780511711909.007

Gibbs AG, Chippindale AK, Rose MR (1997) Physiological mechanisms of evolved desiccation resistance in *Drosophila melanogaster*. J Exp Biol 200:1821–1832

Gomulkiewicz R, Holt RD (1995) When does evolution by natural-selection prevent extinction. Evolution 49:201–207. https://doi.org/10.1111/j.1558-5646.1995.tb05971.x

Gordon DM, Heller NE (2014) The invasive argentine ant *Linepithema humile* (Hymenoptera: Formicidae) in northern California reserves: from foraging behavior to local spread. Myrmecological News 19:103–110

Greene MJ, Gordon DM (2007) Structural complexity of chemical recognition cues affects the perception of group membership in the ants *Linepithema humile* and *Aphaenogaster cockerelli*. J Exp Biol 210:897–905. https://doi.org/10.1242/jeb.02706

Hadley NF (1981) Cuticular lipids of terrestrial plants and arthropods - a comparison of their structure, composition, and waterproofing function. Biol Rev Camb Philos Soc 56:23–47

Heller NE, Sanders NJ, Shors JW, Gordon DM (2008) Rainfall facilitates the spread, and time alters the impact, of the invasive argentine ant. Oecologia 155:385–395. https://doi.org/10.1007/s00442-007-0911-z

Holway DA, Suarez AV, Case TJ (1998) Loss of intraspecific aggression in the success of a widespread invasive social insect. Science 283:949–952

Holway DA, Lach L, Suarez AV, Tsutsui ND, Case TJ (2002) The causes and consequences of ant invasions. Annu Rev Ecol Syst 33:181–233. https://doi.org/10.1146/annurev.ecolsys.33.010802.150444

Howard RW, Blomquist GJ (2005) Ecological, behavioral, and biochemical aspects of insect hydrocarbons. Annu Rev Entomol 50:371–393

Ingleby FC (2015) Insect cuticular hydrocarbons as dynamic traits in sexual communication. Insects 6:732–742. https://doi.org/10.3390/insects6030732

Jackson LL, Baker GL (1969) Cuticular lipids of insects. Lipids 5:239–246

Kolar CS, Lodge DM (2001) Progress in invasion biology: predicting invaders. Trends Ecol Evol 16:199–204. https://doi.org/10.1016/S0169-5347(01)02101-2

Krasnec MO, Breed MD (2013) Colony-specific cuticular hydrocarbon profile in *Formica argentea* ants. J Chem Ecol 39:59–66. https://doi.org/10.1007/s10886-012-0227-2

Liu ZB, Bagnères AG, Yamane S, Wang QC, Kojima J (2001) Intra-colony, inter-colony and seasonal variations of cuticular hydrocarbon profiles in *Formica japonica* (Hymenoptera, Formicidae). Insect Soc 48:342–346. https://doi.org/10.1007/PI00001787

Lowe S, Browne M, Boudjelas S, De Poorter M (2004) 100 of the World's worst invasive alien species vol 12. The invasive species specialist group (ISSG); world conservation union. IUCN

Markin GP (1970) Foraging behavior of the argentine ant in California citrus groves. J Econ Entomol 63:740–744

Martin S, Drijfhout F (2009) A review of ant cuticular hydrocarbons. J Chem Ecol 35:1151–1161. https://doi.org/10.1007/s10886-009-9695-4

Menzel F, Blaimer BB, Schmitt T (2017) How do cuticular hydrocarbons evolve? Physiological constraints and climatic and biotic selection pressures act on a complex functional trait. Proc R Soc Lond Ser B Biol Sci 284:20161727. https://doi.org/10.1098/rspb.2016.1727

Menzel F, Zumbusch M, Feldmeyer B (2018) How ants acclimate: impact of climatic conditions on the cuticular hydrocarbon profile. Funct Ecol 32:657–666. https://doi.org/10.1111/1365-2435.13008

Michelutti KB, Soares ERP, Sguarizi-Antonio D, Piva RC, Suarez YR, Cardoso CAL, Antonialli-Junior WF (2018) Influence of temperature on survival and cuticular chemical profile of social wasps. J Therm Biol 71:221–231. https://doi.org/10.1016/j.jtherbio.2017.11.019

Newell W, Barber TC (1913) The argentine ant. US Department of Agriculture, Bureau of Entomology 122:1–98

Nielsen J, Boomsma JJ, Oldham NJ, Petersen HC, Morgan ED (1999) Colony-level and season-specific variation in cuticular hydrocarbon profiles of individual workers in the ant *Formica truncorum*. Insect Soc 46:58–65. https://doi.org/10.1007/s000400050113

Oksanen J, Kindt R, Legendre P, O'Hara RB (2007) Vegan: community ecology package

Pedersen JS, Krieger MJB, Vogel V, Giraud T, Keller L (2006) Native supercolonies of unrelated individuals in the invasive argentine ant. Evolution 60:782–791

Rajpurohit S, Hanus R, Vrkoslav V, Behrman EL, Bergland AO, Petrov D, Cvacka J, Schmidt PS (2017) Adaptive dynamics of cuticular hydrocarbons in *Drosophila*. J Evol Biol 30:66–80. https://doi.org/10.1111/jeb.12988

Rouault J-D, Marican C, Wicker-Thomas C, Jallon J-M (2004) Relations between cuticular hydrocarbon (HC) polymorphism, resistance against desiccation and breeding temperature; a model for HC evolution in *D. melanogaster* and *D. simulans*. Genetica 120:195–212. https://doi.org/10.1023/b:Gene.0000017641.75820.49

Sakata I, Hayashi M, Nakamuta K (2017) *Tetramorium tsushimae* ants use methyl branched hydrocarbons of aphids for partner recognition. J Chem Ecol 43:966–970. https://doi.org/10.1007/s10886-017-0891-3

Schilman PE, Lighton JR, Holway DA (2005) Respiratory and cuticular water loss in insects with continuous gas exchange: comparison across five ant species. J Insect Physiol 51:1295–1305. https://doi.org/10.1016/j.jinsphys.2005.07.008

Suarez AV, Tsutsui ND, Holway DA, Case TJ (1999) Behavioral and genetic differentiation between native and introduced populations of the argentine ant. Biol Invasions 1:43–53

Suarez AV, Holway DA, Case TJ (2001) Patterns of spread in biological invasions dominated by long-distance jump dispersal: insights from argentine ants. Proc Natl Acad Sci U S A 98:1095–1100

Suarez AV, Holway DA, Liang D, Tsutsui ND, Case TJ (2002) Spatiotemporal patterns of intraspecific aggression in the invasive argentine ant. Anim Behav 64:697–708

Sunamura E, Hatsumi S, Karino S, Nishisue K, Terayama M, Kitade O, Tatsuki S (2009) Four mutually incompatible argentine ant supercolonies in Japan: inferring invasion history of introduced argentine ants from their social structure. Biol Invasions 11:2329–2339. https://doi.org/10.1007/s10530-008-9419-7

Team RC (2018) R: A language and environment for statistical computing. R foundation for statistical computing, http://www.R-project.org, Vienna, Austria

Torres CW, Brandt M, Tsutsui ND (2007) The role of cuticular hydrocarbons as chemical cues for nestmate recognition in the invasive argentine ant (*Linepithema humile*). Insect Soc 54:363–373

Tsutsui ND, Case TJ (2001) Population genetics and colony structure of the argentine ant (*Linepithema humile*) in its native and introduced ranges. Evolution 55:976–985

Tsutsui ND, Suarez AV (2003) The colony structure and population biology of invasive ants. Conserv Biol 17:48–58

Tsutsui ND, Suarez AV, Holway DA, Case TJ (2000) Reduced genetic variation and the success of an invasive species. Proc Natl Acad Sci U S A 97:5948–5953

Tsutsui ND, Suarez AV, Holway DA, Case TJ (2001) Relationships among native and introduced populations of the argentine ant (*Linepithema humile*) and the source of introduced populations. Mol Ecol 10:2151–2161

Tsutsui ND, Suarez AV, Grosberg RK (2003) Genetic diversity, asymmetrical aggression, and recognition in a widespread invasive species. Proc Natl Acad Sci U S A 100:1078–1083

van Wilgenburg E, Sulc R, Shea KJ, Tsutsui ND (2010) Deciphering the chemical basis of nestmate recognition. J Chem Ecol 36:751–758. https://doi.org/10.1007/s10886-010-9812-4

van Wilgenburg E, Felden A, Choe DH, Sulc R, Luo J, Shea KJ, Elgar MA, Tsutsui ND (2012) Learning and discrimination of cuticular hydrocarbons in a social insect. Biol Lett 8:17–20. https://doi.org/10.1098/rsbl.2011.0643

Wagner D, Tissot M, Gordon D (2001) Task-related environment alters the cuticular hydrocarbon composition of harvester ants. J Chem Ecol 27:1805–1819. https://doi.org/10.1023/a:1010408725464

Woodrow RJ, Grace JK, Nelson LJ, Haverty MI (2000) Modification of cuticular hydrocarbons of *Cryptotermes brevis* (Isoptera: Kalotermitidae) in response to temperature and relative humidity. Environ Entomol 29:1100–1107. https://doi.org/10.1603/0046-225X-29.6.1100